

# Electronic properties of chemically modified graphene ribbons

F. Cervantes-Sodi, G. Csányi, S. Piscanec, and A. C. Ferrari\*

Department of Engineering, University of Cambridge, Cambridge, UK

Received 9 May 2008, revised 13 June 2008, accepted 8 July 2008

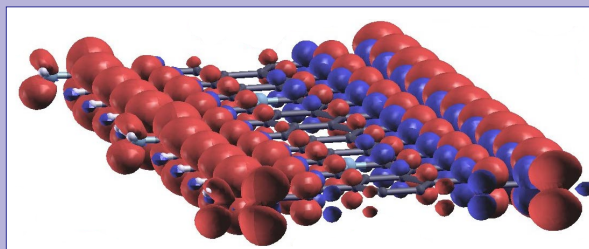
Published online 29 August 2008

PACS 71.15.Mb, 73.20.Hb, 73.22.-f

\* Corresponding author: e-mail acf26@hermes.cam.ac.uk, Phone: +44-1223-748351, Fax: +44-1223-748348

We compare the electronic properties of graphene nanoribbons, with either bulk or edge substitutions, edge functionalization, or chemisorption. Chemical modifications can cause semiconductor-metal transitions, lifting of spin degeneracy, widening of bandgap, or appearance of non-dispersive impurity bands and doping.

(Right) Ferromagnetic spin arrangement on N-bulk substituted+NH<sub>2</sub> edge functionalized zigzag ribbon



© 2008 WILEY-VCH Verlag GmbH & Co. KGaA, Weinheim

**1 Introduction** Graphene nanoribbons (GNRs) are the counterpart of nanotubes in graphene nanoelectronics. Electron confinement opens a bandgap, making them suitable for the realization of devices. Due to the potential technological applications, their electronic structure has been widely investigated [1–27], with particular attention to the factors determining the presence and size of the gap.

Graphene can be identified in terms of number and orientation of the layers by elastic and inelastic light scattering, such as Raman [28–31] and Rayleigh spectroscopies [32,33]. Raman spectroscopy also allows monitoring of doping and defects [28,29,34,35]. Once identified, graphene layers can be processed into ribbons by lithography [36–39].

When GNRs are cut from a single layer, their edges could in general consist of a combination of regions having an armchair or a zigzag geometry [40–43]. If a ribbon is uniquely limited by one of these edges, it is defined either as an armchair GNR (AGNR) or as a zigzag GNR (ZGNR).

Chemical impurities, atomic substitutions and functional groups can be an effective way to modify the electronic properties of both graphene [44] and nanoribbons [23,45] and, in principle, a way to control them. Furthermore, covalently bonded impurities are likely to result

from the production processes. In particular H, O and oxygen containing radicals could be present on the edges or as adsorbates.

Here we consider functionalized, chemisorbed and atomic substituted GNRs. We discuss the interplay between edge localized orbitals and chemical modifications.

**2 Methodology** We perform spin polarized density functional theory (DFT) calculations with the CASTEP code [46]. We use the Perdew-Burke-Ernzerhof gradient corrected functional [47] and ultrasoft pseudopotentials [48], cut-off at 400 eV. Hydrogen terminated ribbons are built from the graphite geometry with an initial C-C distance of 1.42 Å. Geometry optimization is performed for all the modified structures. GNRs are defined by the number of unit cells in the  $x$  and  $y$  directions. E.g., if the ribbon has 6 and 2 rows of atoms in the non-periodic and periodic directions, then it is called the  $6 \times 2$  GNR. The supercell Brillouin zones (BZ) are sampled by Monkhorst-Pack grids of the form  $P \times 1 \times 1$  with  $P$  such that the maximum spacing between  $k$ -points in the periodic direction  $x$  is  $< 0.1 \text{ \AA}^{-1}$ . To simulate isolated GNRs, the in-plane and perpendicular distances between GNRs in adjacent supercells have to be larger than 5.5 Å; 6.5 Å.

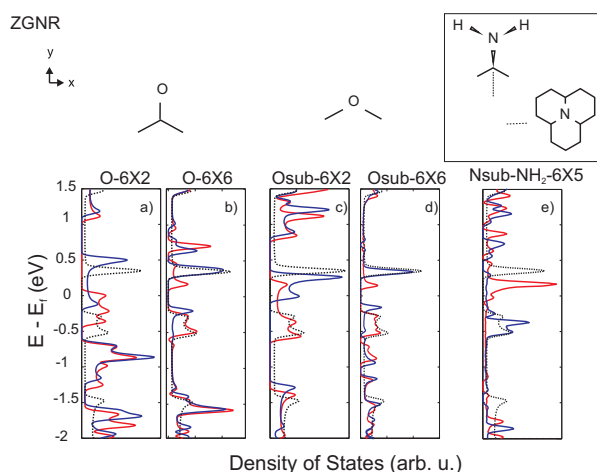


**Figure 1** (color online) Black dotted lines represent the DOS of pristine GNR; spin up and down DOS of the modified GNRs are indicated with red and blue lines. (a),(b) Single sided ketonated  $6 \times 2$ ,  $6 \times 6$  GNRs. (c),(d) Single sided etheration at the edge of the same GNRs. (e)  $\text{NH}_2$  functionalized + N bulk substituted  $6 \times 5$  GNRs.

### 3 Results

**3.1 Zigzag GNRs** have an anti-ferromagnetic (AF) ground state, where electronic states with different spin are highly localized at opposite edges [8, 10]. Two metastable states exist: the first has a ferromagnetic spin arrangement, with a finite total magnetic moment. The second, at higher energy, is non-magnetic [8, 10]. After functionalization, the AF ground state is maintained for most GNRs [45], although in some cases a magnetic moment appears. The effects of functionalization and atomic substitution are shown in Fig. 1,2; chemisorption in Fig. 2.

**ZGNR Single edge functionalization** is studied for  $\text{NH}_2$ ,  $\text{NO}_2$ ,  $\text{OH}$ ,  $\text{COOH}$  and  $\text{O}$  radicals covalently bonded to one of the edges. In all cases, we get a lifting of the spin degeneracy, and a modification of the bandgap, that fingerprint each radical, as shown in Table 1. In Ref. [45] we reported the Density Of States (DOS) for all these structures, while here we focus on the comparison of functionalization via introduction of ketone groups at two different densities, i.e. the  $6 \times 2$  and  $6 \times 6$  ZGNR. The DOS are shown in Fig. 1(a,b). Ketonation -via atomic substitution- at high density ( $6 \times 2$ ) results in a semiconductor-metal transition, while at the chosen lower density configuration ( $6 \times 6$ ) the ribbon recovers its semiconductor character, with a change of bandgap for each spin channel of  $-30\%$  and  $+40\%$ . The AF ground state is substantially preserved upon functionalization for most of the tested radicals. In contrast,  $\text{O}$  eliminates the localization of the corresponding spin in the vicinity of the functionalization site. Thus, the AF arrangement of the spin is lost for high density functionalization, and considerably altered for low density. Furthermore, the integrated spin density changes to  $0.0058$  and  $0.0038 e/\text{\AA}^2$ .

**Edge carbon substitutions** also lift the spin degeneracy. Using ether groups at the same densities considered for ketonation, we observe a similar behavior. The spin degeneracy is lifted: for high density etheration the GNR undergoes a semiconductor-metal transition, while for low it remains semiconducting, with a bandgap change of  $-22\%$  and  $-31\%$  for each spin. In this case the AF spin arrangement is also modified, and the integrated spin densities for the  $6 \times 2$  and  $6 \times 6$  GNRs are  $0.0058$  and  $0.0035 e/\text{\AA}^2$ .

Figure 1(e) plots the  $6 \times 5$  GNR with simultaneous N bulk substitution and  $\text{NH}_2$  single edge functionalization.  $\text{NH}_2$  is placed in the opposite carbon sub-lattice with respect to the N. This aims to alter the electronic state of both sub-lattices, in order to illustrate the high impact that even small modifications can have on the GNR properties. The effect is to flip the relative energy of the AF and ferromagnetic states, resulting in a GNR with a ferromagnetic spin configuration, as shown in the abstract figure, where both edges have a strong spin density of the same sign of  $0.0077 e/\text{\AA}^2$ . This is comparable with the integrated spin density of a clean ZGNR in its metastable ferromagnetic state.

**Edge spin states** of ZGNRs can be altered by any chemical modifications. In Fig. 2(a,b) show the band structure of the one-sided and two-sided ketonated  $6 \times 6$  GNR.

**Table 1** Spin up and down bandgap of modified GNRs;  $F_s$ =Single edge functionalized,  $F_d$ =Double edge functionalized, C=chemisorbed, S=atomic substituted.

type	chemical modification		ribbon	bandgap (eV)	
				up spin	down spin
ZGNR	$F_s$	$\text{NH}_2$	$6 \times 2$	0.42	0.39
	$F_s$	$\text{NO}_2$	$6 \times 2$	0.66	0.28
	$F_s$	$\text{OH}$	$6 \times 2$	0.57	0.49
	$F_s$	$\text{COOH}$	$6 \times 2$	0.62	0.45
	$F_s$	$\text{O}$	$6 \times 2$	metallic	metallic
	$F_s$	$\text{O}$	$6 \times 6$	0.82	0.41
	$F_d$	$\text{O}$	$6 \times 2$	metallic	metallic
	$F_d$	$\text{O}$	$6 \times 6$	0.50	0.50
	$S$	O edge	$6 \times 2$	metallic	metallic
	$S$	O edge	$6 \times 6$	0.45	0.40
	$C$	$\text{OH}$ edge	$6 \times 8$	0.45	0.59
	$C$	$\text{OH}$ bulk	$6 \times 8$	0.59	0.67
AGNR	$F_s$	$\text{NH}_2$	$12 \times 3$	0.64	0.64
	$S$	B edge	$12 \times 3$	0.59	0.59
	$S$	N edge	$12 \times 3$	0.63	0.63
	$S$	B bulk	$12 \times 3$	metallic	metallic
	$S$	N bulk	$12 \times 3$	metallic	metallic
	$C$	$\text{OH}$ bulk	$12 \times 1$	0.91	0.91
	$C$	$\text{OH}$ bulk	$12 \times 3$	0.84	0.84
	$C$	H bulk	$12 \times 3$	0.81	0.81

Spin degeneracy lifting only happens for single edge functionalization, while the double edge has a fully spin degenerated state. In both cases, the final state is a semiconducting GNR with hybrid orbitals, localized in the vicinity of the impurity, as shown in Fig. 2. In particular, for double sided functionalization, the hybrid orbitals are  $\gamma$  and  $\delta$ .  $\gamma$  is 0.5eV away from the bottom of the conduction band, defined by edge orbitals indicated by  $\beta$  in Fig.2(b).

Figure 2 also shows the different ways in which OH adsorption on the GNR surface modifies the bandgap, depending on the OH relative position with respect to the edges. Adsorption plays a fundamental role in determin-

ing the electronic properties of graphene and GNRs, and it is of major technological interest. In pristine ribbons, C atoms closer to the edge are more reactive, and present a strong localization of the spin density at the ribbon edges; the edge states define the bandgap. ZGNRs are more stable upon edge adsorption, indeed the difference in stability between the two cases shown in Figs.2(c,d) is  $\sim 0.62$  eV. Due to the localization of the spin density on the ribbon edges, edge and bulk chemisorption modify differently the band structure. The gray region in Figs. 2(c,d) shows this. The modified ribbon has 5(4) spin up(down) modified bands, while the pristine has 4 spin degenerated bands. The electron provided by the O unpaired bond in the radical sits on the top of the valence band. The chemisorbed OH generates an accumulation region of spin up density (red) in its vicinity, opposite to the down spin (blue) of the carbon sublattice to which it is bonded. For both cases, the extra band hybridizes in different degrees with the edge states at the top  $\sim 1$ eV of the valence band (we include the top two  $\alpha$  and  $\beta$  spin up bands, and their corresponding orbitals, shown in red in Figs. 2(c,d)). For both edge and bulk an empty band ( $\beta$ , blue in Figs. 2(c,d)) defines the bottom of the conduction band. In the bulk case, its associated spin orbital is completely localized in the vicinity of the impurity, while in the edge case, it hybridizes with the edge state. These ribbons present a half-semiconductor behavior with different bandgap for each spin.

**3.2 Armchair GNRs** have a bandgap originating from quantum confinement [8] and, unlike ZGNRs, do not have edge states near the bandgap. Thus, the effect of edge modifications is expected to be weaker than in ZGNRs.

**Functionalization** of AGNRs is shown in Fig3(a), where  $\text{NH}_2$  is covalently bonded to an edge atom of the  $12 \times 3$ AGNR. An impurity level appears 1.5eV below the valence band. The gap is almost invariant with no lift of spin degeneracy.

**Atomic Substitution** on the edges introduces impurity levels very far from the Fermi energy, and the electronic properties are unchanged. N edge atoms are attached with very localized chemical bonds in an  $\text{sp}^3$  configuration. This promotes a deep state in the valence band, occupied by the extra electron carried by the N. On the contrary, N in the bulk is in an  $\text{sp}^2$  configuration, resulting in delocalized states in the conduction band. Since no new states are formed in the valence band, the extra electrons coming from N have to be allocated to what was the conduction band of the pristine GNR, with a consequent shift of the Fermi energy that promotes a *semiconductor-metal* transition. A specular behavior happens for B: edge doping does not change the electronic configuration and bulk doping promotes a *semiconductor-metal* transition.

**Chemisorption** The main changes following OH and H chemisorbed radicals are the widening of the bandgap and the appearance of a half-occupied, spin-degenerated, non-dispersive impurity band in the middle of the gap. The gap widening is a significant result, and it

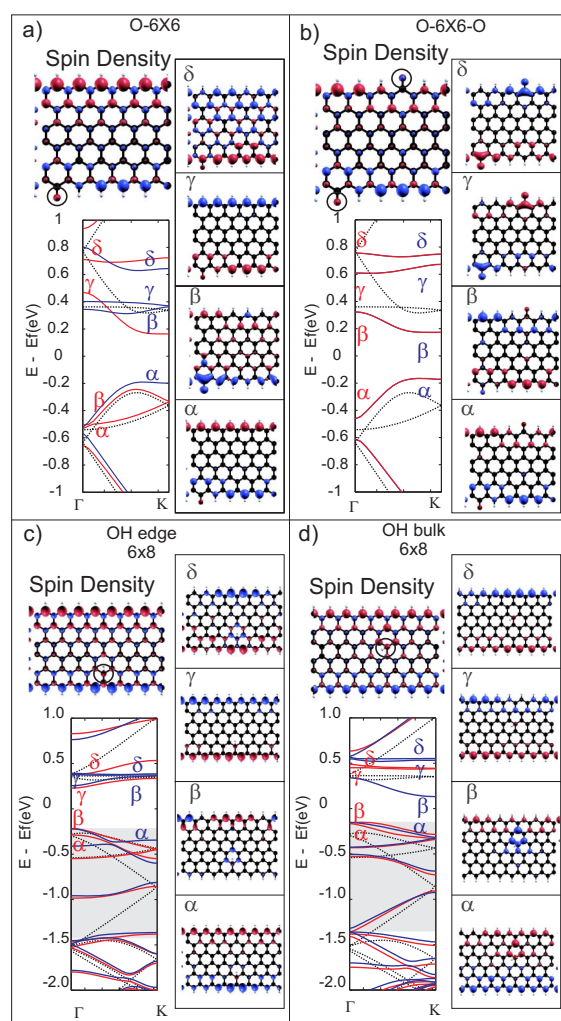


**Figure 2** (color online) Bands of a pristine ribbon (black dotted line) and of up (red) and down (blue) spin channels for (a) single edge and (b) double edge functionalized  $6 \times 6$ ZGNR. The up (down) spin orbitals corresponding to the bandgap edges and the total spin density are plotted in red (blue) in the right and top of each band structure, showing the localization of the gap bands.(c),(d) bands and edge orbitals of OH chemisorbed close to edge and in the bulk.

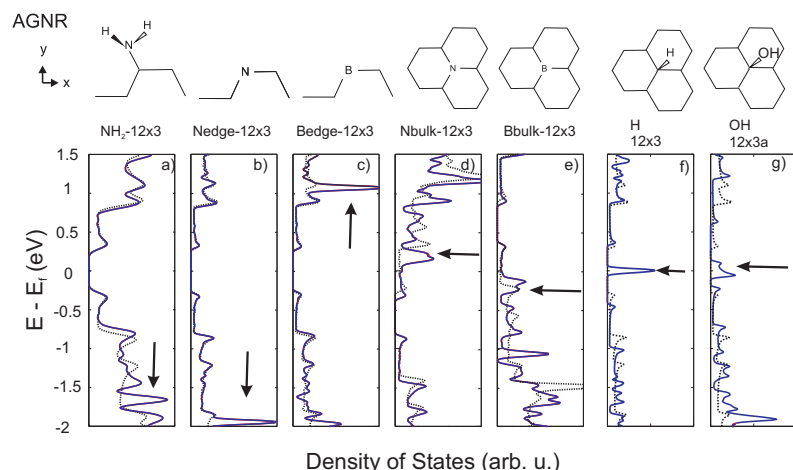


**Figure 3** (color online) (a)  $\text{NH}_2$  functionalization, (b) N and (c) B edge substitution, (d) N and (e) B bulk substitution, (f) H and (g) OH chemisorption on the  $12 \times 3$  AGNR. Arrows indicate the impurity bands. The DOS of the clean GNR is shown with black dotted lines.

could explain why, thus far, the measured gap in experimental ribbons [36] was always bigger than that predicted by electron confinement [8]. More generally, it shows that chemisorption provides a route to engineer and control the bandgap, without the need of cutting extremely small GNRs, as required by pure electron confinement. We believe this will have significant technological implications. The impurity band is indicated by the arrows in Fig. 3(f,g), and the corresponding orbital is highly localized in the vicinity of the adsorbates. This is similar to what reported for H chemisorption on bulk graphene [49,50], which creates a gap, and an impurity band in the middle [49,50]. However, in graphene the chemisorption induces a magnetic moment of  $1\mu_B$ , which is not present in chemisorbed AGNRs. The strong localization of the orbitals associated with H and OH, and their position near the middle of the bandgap could make them behave in a similar way to doped semiconductors.

**4 Conclusions** The GNRs electronic properties can be altered through chemical modifications. Edge functionalization, atomic substitution and chemisorption of different radicals can induce semiconductor-metallic transitions, half semiconducting states and electronic doping. This suggests that chemical modifications will be key to engineer technologically relevant GNRs [44].

**Acknowledgements** F.C.S. acknowledges funding from CONACYT Mexico, S.P. from Pembroke College, A.C.F. from The Royal Society and The Leverhulme Trust.

## References

- [1] M. Fujita et al., *J. Phys. Soc. Jpn.* **65**, 1920 (1996).
- [2] Y. Miyamoto et al., *Phys. Rev. B* **59**, 9858 (1999).
- [3] K. Wakabayashi et al., *Phys. Rev. B* **59**, 8271 (1999).
- [4] K. Sasaki et al., *Appl. Phys. Lett.* **88**, 113110 (2006).
- [5] M. Fujita et al., *J. Phys. Soc. Jpn.* **66**, 1864 (1997).
- [6] K. Nakada et al., *Phys. Rev. B* **54**, 17954 (1996).
- [7] K. Nakada et al., *J. Phys. Soc. Jpn.* **67**, 2388 (1998).
- [8] Y. W. Son et al., *Phys. Rev. Lett.* **97**, 216803 (2006).
- [9] H. Lee et al., *Phys. Rev. B* **72**, 174431 (2005).
- [10] L. Pisani et al., *Phys. Rev. B* **75**, 064418 (2007).
- [11] S. Okada and A. Oshiyama, *Phys. Rev. Lett.* **87**, 146803 (2001).
- [12] Y. W. Son et al., *Nature* **444**, 347 (2006).
- [13] L. Yang et al., *Phys. Rev. Lett.* **99**, 186801 (2007).
- [14] D. Prezzi et al., arXiv:0706.0916v1.
- [15] O. Hod et al., *Nano Lett.* **7**, 2295 (2007).
- [16] E. J. Kan et al., *Appl. Phys. Lett.* **91**, 243116 (2007).
- [17] E. Rudberg et al., *Nano Lett.* **7**, 2211 (2007).
- [18] O. Hod et al., *Phys. Rev. B* **77**, 035411 (2008).
- [19] I. Martin, Y. M. Blanter, arXiv:0705.0532v2.
- [20] D. A. Areshkin et al., *Nano Lett.* **7**, 204 (2007).
- [21] D. Gunlycke et al., *Appl. Phys. Lett.* **90**, 142104 (2007).
- [22] V. Barone et al., *Nano Lett.* **6**, 2748 (2006).
- [23] T. B. Martins et al., *Phys. Rev. Lett.* **98**, 196803 (2007).
- [24] B. Huang et al., arXiv:0708.1795v1.
- [25] H. Zheng et al., *Phys. Rev. B* **75**, 165414 (2007).
- [26] Z. Chen et al., *Physica E* **40**, 228 (2007).
- [27] Y. Zhang et al., *Appl. Phys. Lett.* **86**, 073104 (2005).
- [28] S. Pisana et al., *Nature Mater.* **6**, 198 (2007).
- [29] C. Casiraghi et al., *Appl. Phys. Lett.* **91**, 233108 (2007).
- [30] A. C. Ferrari et al., *Phys. Rev. Lett.* **97**, 187401 (2006).
- [31] S. Piscanec et al., *Phys. Rev. Lett.* **93**, 185503 (2004).
- [32] C. Casiraghi et al., *Nano Lett.* **7**, 2711 (2007).
- [33] P. Blake et al., *Appl. Phys. Lett.* **91**, 063124 (2007).
- [34] A. C. Ferrari, *Solid State Commun.* **143**, 47 (2007).
- [35] A. Das et al., *Nature Nanotechnol.* **3**, 210 (2008).
- [36] M. Y. Han et al., *Phys. Rev. Lett.* **98**, 206805 (2007).
- [37] C. Berger et al., *Science* **312**, 1191 (2006).
- [38] X. Lu et al., *Appl. Phys. Lett.* **75**, 193 (1999).
- [39] M. C. Lemme et al., *IEEE Electron Device Lett.* **28**, 4 (2007).
- [40] Y. Niimi et al., *Phys. Rev. B* **73**, 085421 (2006).
- [41] Y. Kobayashi et al., *Phys. Rev. B* **71**, 193406 (2005).
- [42] F. Sols et al., *Phys. Rev. Lett.* **99**, 166803 (2007).
- [43] Y. Niimi et al., *Appl. Surf. Sci.* **241**, 43 (2005).
- [44] T. J. Echtermeyer et al., arXiv:0805.4095; 0712.2026.
- [45] F. Cervantes-Sodi et al., *Phys. Rev. B* **77**, 165427 (2008).
- [46] S. J. Clark et al., *Z. Kristallogr.* **220**, 567 (2005).
- [47] J. P. Perdew et al., *Phys. Rev. Lett.* **77**, 3865 (1996).
- [48] D. Vanderbilt, *Phys. Rev. B* **41**, 7892 (1990).
- [49] O. V. Yazyev and L. Helm, *Phys. Rev. B* **75**, 125408 (2007).
- [50] E. J. Duplock et al., *Phys. Rev. Lett.* **92**, 225502 (2004).